THE CHEMICAL RECORD

Casting New Physicochemical Light on the Fundamental Biological Processes in Single Living Cells by Using Raman Microspectroscopy

VENKATESH KALIAPERUMAL[1] AND HIRO-O HAMAGUCHI*[1,2]
[1]Department of Chemistry, School of Science, The University of Tokyo, Hongo 7-3-1 Bunkyo-ku Tokyo,113-0033 (Japan)
[2]Institute of Molecular Science and Department of Applied Chemistry, National Chiao Tung University, 1001 Ta Hsueh Road, Hsinchu 300 (Taiwan)
E-mail: hhama@nctu.edu.tw

Received: March 18, 2012
Published online: November 5, 2012

ABSTRACT: This Personal Account highlights the capabilities of spontaneous Raman microspectroscopy for studying fundamental biological processes in a single living cell. Raman microspectroscopy provides time- and space-resolved vibrational Raman spectra that contain detailed information on the structure and dynamics of biomolecules in a cell. By using yeast as a model system, we have made great progress in the development of this methodology. The results that we have obtained so far are described herein with an emphasis placed on how three cellular processes, that is, cell-division, respiration, and cell-death, are traced and elucidated with the use of time- and space-resolved structural information that is extracted from the Raman spectra. For cell-division, compositional- and structural changes of various biomolecules are observed during the course of the whole cell cycle. For respiration, the redox state of mitochondrial cytochromes, which is inferred from the resonance Raman bands of cytochromes, is used to evaluate the respiration activity of a single cell, as well as that of isolated mitochondrial particles. Special reference is made to the "Raman spectroscopic signature of life", which is a characteristic Raman band at 1602 cm^{-1} that is found in yeast cells. This signature reflects the cellular metabolic activity and may serve as a measure of mitochondrial dysfunction. For cell-death, "cross-talk" between the mitochondria and the vacuole in a dying cell is suggested. **DOI 10.1002/tcr.201200008**

Keywords: lipids; living cells; mitochondria; Raman microspectroscopy; yeast

1. Introduction

The evolution of a new microscopic technique always advances our understanding of life. Raman microspectroscopy, which is an alliance of Raman spectroscopy and optical confocal microscopy, is no exception. It offers new possibilities for the in vivo observation of dynamical biological processes at the molecular level. Needless to say, all biological processes, including birth, life, and death, result from dynamic interactions between ensembles of molecules in cells, tissues, organs, and organ systems. Raman microspectroscopy provides time- and space-resolved Raman spectra, or "molecular fingerprints", that contain detailed and otherwise-unobtainable information on molecules that take part in these biological processes. In addition, Raman microspectroscopy offers the advantage of the label-free monitoring of molecules in a living cell, which is not

feasible with other existing live-cell microscopic techniques. It is also suitable for exploratory studies of unknown molecular species that play important roles in fundamental biological processes.

The application of Raman microspectroscopy to a single cell was pioneered almost two decades ago by Puppels et al., who reported the Raman spectrum of human lymphocyte cell under a microscope. They were able to assign the many observed Raman bands to known biomolecules, like DNA and proteins.[1] Following this work, there have been a number of reports on the Raman microspectroscopy of "living" cells. However, the problem of photodegradation of biomolecules in living cells has not been meticulously addressed. It was not clear whether these "living" cells were really living or how high/low their bioactivities were, because life and death at the molecular level was not well-defined. We reported the first Raman spectroscopic observation of a dividing cell that was without-doubt living.[2] A set of time- and space-resolved Raman spectra of the central part of a single living fission-yeast cell was successfully measured to show highly dynamical nature of the molecular compositions and distributions as cell cycle proceeded from the G1 through the S, G2, and M phases. Since then, we have been using yeasts for studying selected fundamental biological processes in a living cell by Raman microspectroscopy.

Yeasts are eukaryotic cells of 5–10 μm in size and they possess most of organelles that exist in higher plant- and animal cells. They are used as model organisms in many biological and biochemical studies. Their size of 5–10 μm facilitates the space-resolved observation of their constituent organelles separately by using Raman microspectroscopy (for spatial resolution, see the Experimental Details section). Fission yeast *Schizosaccharomyces pombe* divides symmetrically with the formation of a septum; its cell cycle takes typically a few hours. A measurement time of 1–100 s is long enough to time-resolve the process of mitosis of a single cell (for time-resolution, see the Experimental Details section). By using green-fluorescent protein (GFP) that was targeted towards either the nucleus or the mitochondria, we are able to obtain Raman spectra of the nucleus and mitochondria during various phases of the cell cycle.[3] The formation and maturation of the cell septum is also traced by Raman microspectroscopy. GFP-tagged mitochondria from aerobically respiring fission-yeast cells co-localize with a unique Raman peak at 1602 cm^{-1}, which we call the "Raman spectroscopic signature of life".[4] The behavior of this peak in the presence of respiratory inhibitors and oxidative stress is discussed in detail below, along with the probable contributing molecules to this signature. The rate of decrease in intensity of this peak may serve as a measure of mitochondrial dysfunction in a single cell.

Mitochondrial respiration is studied by quantifying the resonance Raman intensities of mitochondrial cytochromes.[5,6] The spectrum of isolated yeast mitochondria shows a quantifiable difference in the redox state of the cytochrome upon the induction of respiratory activity. Thus, the assessment of respiratory activity from the cytochrome redox state is feasible by using a small amount of isolated mitochondria in the focal volume of a confocal Raman microspectrometer. We can now quantify the respiratory activity of a single cell, which has hitherto not been feasible by using any other technique. The dynamics of cell-death has been investigated in budding yeast, *Saccharomyces cerevisiae*. Starvation-induced cell-death is associated with the disappearance of the 1602 cm^{-1} peak, followed by the appearance of a vacuolar dancing body that is composed

Kaliaperumal Venkatesh was born in 1976 in Pondicherry, India. He received his bachelors (MBBS) and doctoral degrees (MD) in Clinical Microbiology from the JIPMER, India. His passion for understanding mitochondrial physiology and pathophysiology in living cells gave him an opportunity to work with Dr. Annapoorni Rangarajan (2005–2009) at the Indian Institute of Science and with Professor Hiro-o Hamaguchi at the University of Tokyo (2009–2012). He has received the Gold Medal from Pondicherry University, a DBT-Post doctoral fellowship, as well as Junior Research Fellowships from the CSIR and the ICMR. His research interests include the applications of vibrational spectroscopy in biology and medicine.

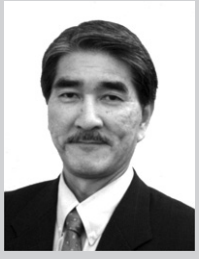

Hiro-o Hamaguchi received his DSc in physical chemistry from the University of Tokyo in 1975. In 1990, he became a Laboratory Head at the Kanagawa Academy of Science and Technology. From 1997 until 2012, he was a Professor of Chemistry at the University of Tokyo. He is currently a Chair Professor at the Department of Applied Chemistry, National Chiao Tung University, Taiwan. His recent research efforts have been directed toward the elucidation of complicated molecular systems, including solutions and liquids, ionic liquids, as well as living cells and human organs, by using time- and space-resolved vibrational spectroscopy. He has received the Meggers Award (2005), the Spectroscopical Society of Japan Award (2006), the Chemical Society of Japan Award (2009), and the TRVS Award (2009).

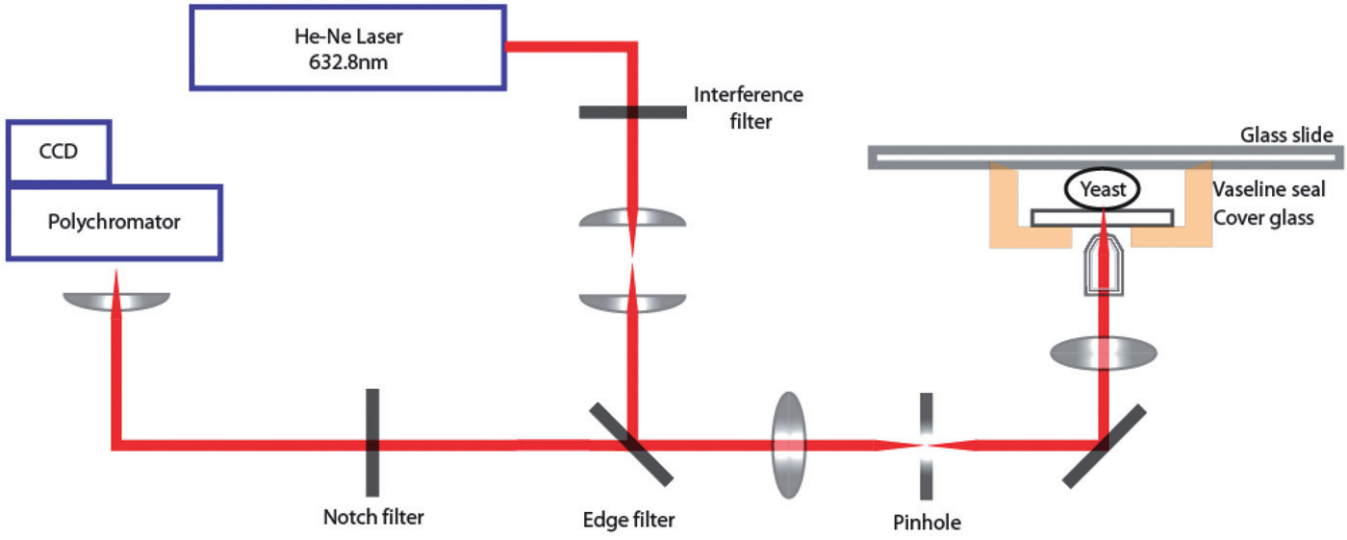

Fig. 1. Schematic diagram of the confocal Raman microspectroscopic system.

of polyphosphates. A few of the fundamental biological processes in a unicellular organism are thus cast in the new light of physical chemistry by using in vivo Raman microspectroscopy.

This Personal Account is not meant to be a comprehensive review of Raman spectroscopy of living cells. Rather, it focuses on the potential of time- and space-resolved Raman microspectroscopy for studying living cells, by using yeast as a prototype model system.

2. Experimental Details

Time- and space-resolved Raman spectra were recorded on a laboratory-made confocal multichannel Raman microspectrometer (Fig. 1). The 532.8 nm line of a Nd :YVO4 laser or the 632.8 nm line of a He-Ne laser were used for Raman excitation. The laser beam was introduced into the microscope with an edge filter that reflected the exciting laser line but transmitted the Raman-scattered light. A 100X oil-immersion objective with NA = 1.3 was used to focus the laser beam to about 1 μm onto a yeast cell that was either attached to a bottom dish that was coated with Concanavalin A or placed between a glass slide and a cover slip.

Vaseline was used to seal the sample to avoid the evaporation of water when the sandwiching method was used. The laser power at the sample was 1–4 mW. The back-scattered Raman signal was collected by using the same objective, passed through a 100 μm pinhole, transmitted through an edge filter and a notch filter (to eliminate Rayleigh scattering), focused into a polychromator, and detected by a thermoelectrically cooled (–70°C) CCD detector. Spatial resolution of 300 nm in the lateral direction and 1.7 μm in the axial direction were achieved. The acquisition time of the spectroscopic data varied from 1 s to 300 s. For the Raman-mapping measurements, integrated Raman intensities were collected for 1 or 2 s from each position of the laser spot whilst the cell was horizontally translated by a piezoelectric stage with a 0.5 μm step in both the *x* and *y* directions. Scanning of the entire cell took between 1 and 20 min.

3. Dynamics of Cell-Division

3.1. The Cell Cycle of Fission Yeast

The cell cycle of fission yeast as a model organism has been extensively studied and characterized into four phases, namely the G1 (gap1), S (synthetic), G2 (gap2), and M (mitotic) phases (Fig. 2).[7] In yeast, the G1 and S phases are often indistinguishable from each other. Under typical culture conditions, it takes a few hours for fission yeast to complete its cell-division. However, it has been found that 4 mW irradiation by a He-Ne laser results in a considerable slowdown of the cell cycle, whilst no appreciable change in the cell cycle is observed with 1 mW irradiation. The G2 phase is the longest phase and many cells usually exist in this phase. The nuclear DNA of the yeast undergoes replication during the S phase. The double copy of the DNA segregates during the M phase and a septum appears in the middle of the cell that divides the cell into two daughter cells. The septum gradually matures and develops into a cell wall, thus completely separating the two daughter cells.

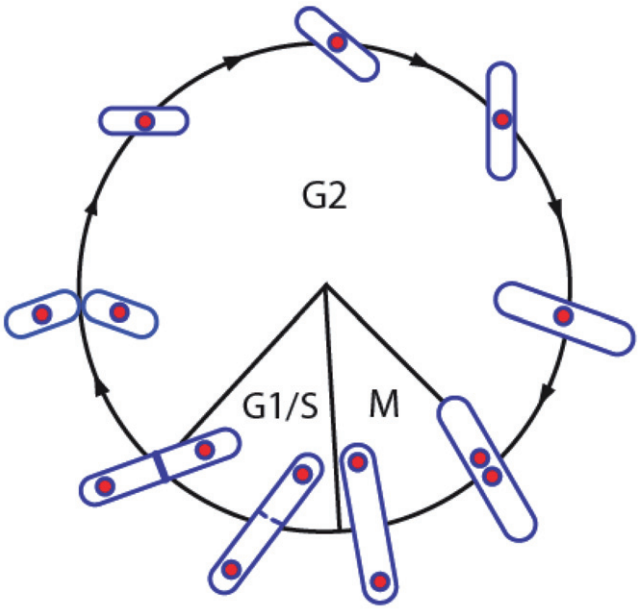

Fig. 2. Schematic diagram of the cell cycle of fission yeast, which shows morphologically distinct G1/S, G2, and M phases.

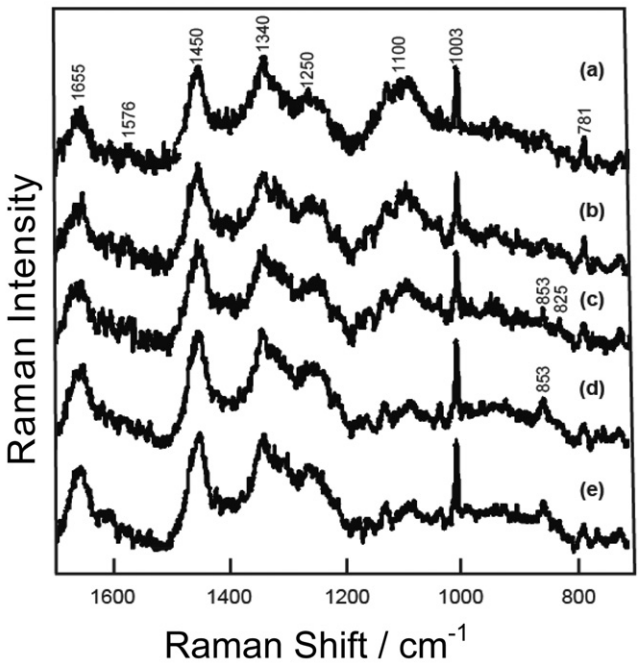

Fig. 3. Raman spectra of a fission-yeast nucleus during various stages of the cell cycle: (a) early G2 phase, (b) late G2 phase, (c) M phase, (d) early G1/S phase, and (e) late G1/S phase.

3.2. Raman Spectra of a Nucleus

The DNA/RNA/protein ratio from an isolated *S. pompe* nucleus was found to be 1:9.4:115.[8] Accordingly, we predominantly find protein bands in the Raman spectra of nuclei (Fig. 3).[3] The amide I and amide III modes of the main chain are located at 1655–1660 cm^{-1} and 1250–1300 cm^{-1}, respectively.[9] The breathing mode of the phenylalanine residue is found at 1003 cm^{-1}. The CH-bend modes of the aliphatic chain are at 1450 cm^{-1} and 1340 cm^{-1}. A broad band that is centered at 1100 cm^{-1} points to a structural change in the hydrocarbon chain and can sensitively reflect the lipid-protein interactions.[10] The doublet bands at 853 cm^{-1} and 825 cm^{-1} are assigned to the Fermi resonance between a totally symmetric ring-breathing mode and the first overtone of an out-of-plane ring-vibration of tyrosyl residues.[11] Hydrogen bonding, tyrosine phosphorylation, and the hydrophobicity of the protein environment are known to influence the intensity ratio of these peaks.[11–13] Weak bands from the nucleic acids are found at 781 cm^{-1} and 1576 cm^{-1}.[14]

The double copy and the closely packed nature of the chromatid DNA in the late G2 and M phase (Fig. 3a and 3b) is reflected in the higher intensity of the band at 781 cm^{-1} when normalized to the protein phenylalanine peak at 1003 cm^{-1}. The Fermi doublet of tyrosine residue at 853 cm^{-1} and 825 cm^{-1} indicates the presence of unphosphorylated-tyrosine-rich proteins in the M-phase nucleus (Fig. 3c). We hypothesize that this feature indicates the predominant presence of an unphosphorylated-tyrosine protein called $p34^{cdc2}$ during this phase. It has been established that, in all eukaryotic cells, cell-cycle entry into the M phase is associated with $p34^{cdc2}$ dephosphorylation.[15, 16] This protein is also the most-abundant phosphotyrosine-containing protein and its phosphorylation status is subjected to cell-cycle regulation in a human cancer cell-line.[17] The presence of a Fermi tyrosine doublet (the unphosphorylated form of the protein) during the M phase correlates with cell-cycle regulation. During the G1/S phase, we find a decrease in the intensity of the 825 cm^{-1} band (Fig. 3d and 3e). This decrease in the low-wavenumber component can be explained by phosphorylation of the nuclear $p34^{cdc2}$ tyrosine residues during this phase. Tyrosine residues buried in a hydrophobic environment of protein or lipid may also contribute to this decrease in the low-wavenumber component. Although there are changes in the protein bands, which reflect structural changes in the protein, these bands needs to be deconvoluted and interpreted cautiously. The broad band at 1100 cm^{-1} shows marked changes on going from the G2 and M phases (Fig. 3a and 3c) to the G1/S phase (Fig. 3d and 3e). It is likely that this band provides more information about the lipid-protein interaction upon detailed analysis.

3.3. Raman Spectra of the Septum and Cell Wall

During the division of a yeast cell into two daughter cells, a primary septum first appears in the center of the cell, which

 The Chemical Record, Vol. 12, 567–580 (2012)

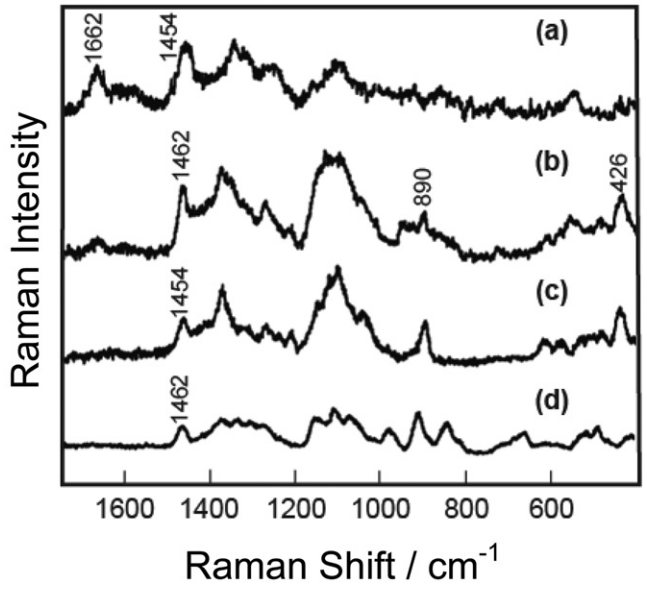

Fig. 4. Raman spectra of (a) the primary septum, (b) mature septum, (c) model compound β-1,3-glucan, and (d) mannan.

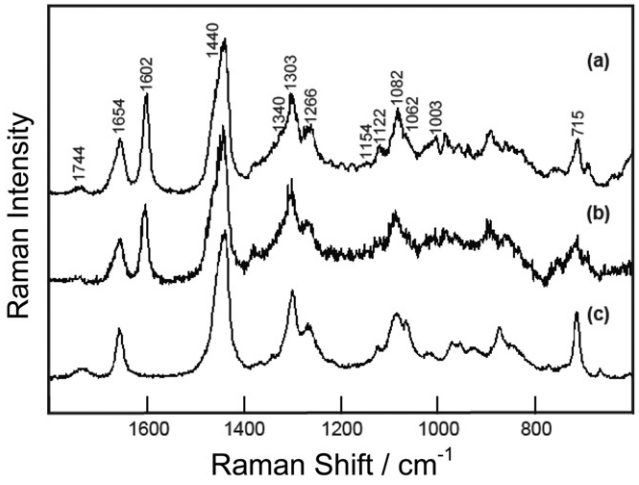

Fig. 5. Raman spectra of (a) lipids from a living yeast cell, (b) isolated mitochondria, and (c) phosphatidylcholine.

gradually matures to form a complete cell wall that divides both the cells. Time-resolved spectra that are obtained from the center of the cell give information on the chemical composition of the cell septum and its transformation during maturation. Fig. 4 compares the Raman spectra of primary (Fig. 4a) and mature septa (Fig. 4b) with those of two model carbohydrates that are known to exist in the septum, β-1,3-glucan (Fig. 4c) and mannan (Fig. 4d).[3] The Raman spectra of the septum show peaks that are assigned to carbohydrates. From a normal-mode analysis of the disaccharides, the presence of a reducing pyranose ring in the primary septum (Fig. 4a) is inferred from a peak at 1454 cm^{-1}, which is assigned to the CH-bend vibration of the CH_2OH group.[18,19] The mature septum shows a band at 1462 cm^{-1}, which is assigned to the same vibration in non-reducing pyranose rings (Fig. 4b). The CO stretch of glycosidic linkage at 890 cm^{-1} is conspicuous in the mature septum.[18,19] These observations suggest an increase in cross-linking during the maturation of the primary septum. Bands in the 1050–1150 cm^{-1} region are from the C-C and C-O stretching modes of the pyranose rings.[18,19] The C-C-C and C-C-O bending mode is located at 426 cm^{-1}.[18,19] Besides polysaccharides, the amide I band at 1662 cm^{-1} is also observed in both primary and mature septa.

3.4. Raman Spectra of Lipids

Under the off-resonance conditions with the 632.8 nm He-Ne laser line, intracellular lipids show strong and distinct Raman bands. Fig. 5 shows the Raman spectra of a lipid-rich region in a living yeast cell (Fig. 5a), in isolated mitochondria (Fig. 5b), and in a prototype phospholipid phosphatidylcholine (Fig. 5c). The Raman spectra in Fig. 5a and 5b closely resemble that of phosphatidylcholine in Fig. 5c.[3] The peak at 1654 cm^{-1} is ascribed to the C=C stretch of the *cis* CH=CH linkage of unsaturated lipid chains.[20] The in-plane C=C-H bend of the *cis* CH=CH linkage shows a peak at 1266 cm^{-1}. The strong peak at 1440 cm^{-1} is assigned to the CH-bending modes, including CH_2 scissors and CH_3 degenerate deformation of the hydrocarbon chain.[20] Another strong peak at 1303 cm^{-1} is assigned to the in-phase CH_2-twist mode.[20] The 1744 cm^{-1} band is due to the C=O stretch of ester linkage.[20] The 1000–1150 cm^{-1} region reflects the skeletal C-C-stretching modes, which are sensitive to the conformation of the hydrocarbon chain.[21] The bands at 1062 cm^{-1} and 1122 cm^{-1} are the out-of-phase and in-phase modes of the all-*trans* chain, whilst the band at 1082 cm^{-1} refers to the *gauche* conformation.[22,23] The ratio of *gauche*/*trans* conformations of the lipids is high and resembles DOPC (1,2-dipalmitoyl-sn-glycero-3-phosphocholine) in the liquid-crystal phase. This fact indicates that lipids in an aerobically cultured living yeast cell are in a less-ordered state.[24] The phospholipid head-group gives a band at around 715 cm^{-1}.[20,25]

We originally assigned these strong lipid signals to mitochondria in a living yeast cell because the spatial distribution of these signals showed good agreement with the GFP image of the mitochondria.[3] The agreement between the two spectra in Fig. 5a and Fig. 5b is consistent with this assignment. However, it later turned out that lipid bodies also show a Raman spectrum that is almost identical to those in Fig. 5a and 5b.[26] The doubly folded mitochondrial membranes are rich in phospholipids, whereas lipid particles are rich in neutral lipids,

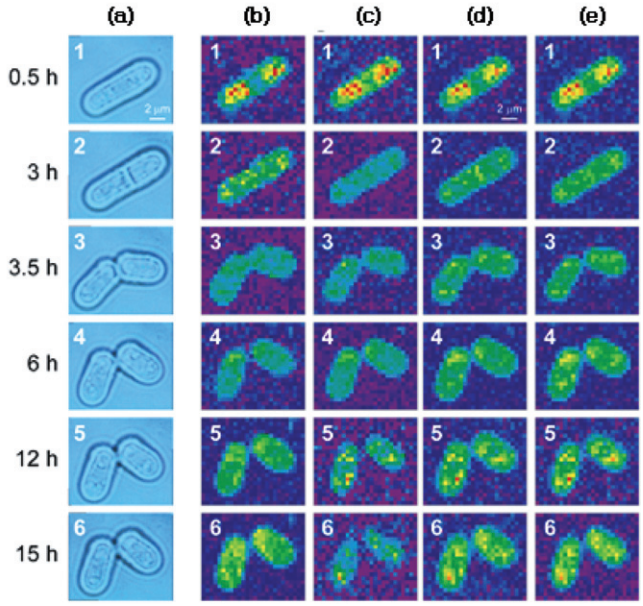

Fig. 6. Time-resolved Raman mapping of a dividing fission-yeast cell: (a) optical image and Raman images at (b) 1655 cm^{-1}, (c) 1602 cm^{-1}, (d) 1440 cm^{-1}, and (e) 1301 cm^{-1}.

namely, triacylglycerol and sterol ester. Cellular fractionation studies have shown that a lipid-particle fraction contains mitochondrial proteins and that a mitochondrial fraction consists of proteins from lipid bodies.[27] These observations imply close physical- and functional interactions between the lipid particles and the mitochondria. The current resolution of Raman microspectroscopy cannot distinguish mitochondria from lipid particles if they are in close proximity to one another. The origin and importance of the 1602 cm^{-1} band is discussed below.

In addition to the many peaks that are assigned to lipids, we also observe an intense and sharp band at 1602 cm^{-1} in the Raman spectrum of a living yeast cell (Fig. 5a). As discussed in detail in the following section, we found that the intensity of this band sharply reflects the metabolic activities of living yeast cells. Accordingly, we call this band the "Raman spectroscopic signature of life" in yeast cells. During the cell cycle, the intensity of this band at 1602 cm^{-1} changes markedly with respect to the phenylalanine peak at 1003 cm^{-1} (data not shown), which probably reflects an increase in the mitochondrial activity and energetic needs of the cells during the M and S phases. We have also shown the existence of this 1602 cm^{-1} Raman band in isolated mitochondria in vitro (Fig. 5b).[28] Cultured tobacco cells also show the presence of this 1602 cm^{-1} Raman band.[29] Independently, The band at 1602 cm^{-1} has also been observed for rat liver tissues,[30] human cancer cells (HeLa), lymphocytes, mesenchymal stem cells, and bovine cartilage cells.[31]

It has been found that, in a resting-phase G2 cell, the concentration of lipids is high but that it drops suddenly with the formation of a septum (Fig. 6).[28] When the cell proceeds towards cell-division, new membranes are synthesized, which may well be reflected by the drop in the concentration of stored lipids. The cell-cycle-dependent distribution of the "Raman spectroscopic signature of life" at 1602 cm^{-1} closely follows the distribution of cellular lipids. Raman-mapping experiments with higher time-resolution will shed more light on the molecular details of the cell cycle, in particular, in terms of lipid concentration.

4. Dynamics of Respiration

4.1. The Redox States of Cytochromes and their Respiration Activity

In eukaryotic cells, respiration takes place in the mitochondria. A mitochondrion is a double-membrane-bound organelle that is rich in lipids. The inner membrane of mitochondria harbors protein complexes that play key roles in respiration, including proteins that contain cytochrome *b* and cytochrome *a*. The energy from food is first transformed into a proton gradient across the mitochondrial membranes through the action of these complexes (called electron transport) and later converted into ATP. The electron-transport chain involves two mobile carriers, ubiquinone and cytochrome *c*. The cytochromes have strong heme absorptions in the green spectroscopic region and a micromolar physiological concentration inside a single cell is easily detected by resonance Raman scattering with excitation at 532 nm.[5,6,32] Fig. 7 shows resonance Raman spectra of cytochromes *b* and *c* in their two redox states, that is, their reduced- and oxidized states, that were obtained from chemically prepared standard solutions.

Cytochrome *b* shows specific bands at 1338 cm^{-1} and 1303 cm^{-1}, which are common to both the reduced- and oxidized forms. The reduced form of cytochrome *c* shows a specific band at 604 cm^{-1}. The band at 1313 cm^{-1} is common to both the reduced- and oxidized forms of cytochrome *c*. The Raman peak at 1638 cm^{-1} is a marker band for the oxidized forms of both cytochromes *b* and *c*. Fig. 8 compares the Raman spectra (excited at 532 nm) of mitochondria in a living budding yeast cell (Fig. 8a), isolated yeast mitochondria in a substrate-depleted respiration-inactive state (Fig. 8b), and isolated yeast mitochondria in an active state. All of the five key bands described above are found in these spectra, which shows that cytochromes in physiological concentrations are indeed observed by resonance Raman scattering with clear indications of their redox states. The marker band at 1638 cm^{-1} shows that the oxidized forms of the cytochromes do not exist in mitochondria in a living cell but that they do exist in the isolated

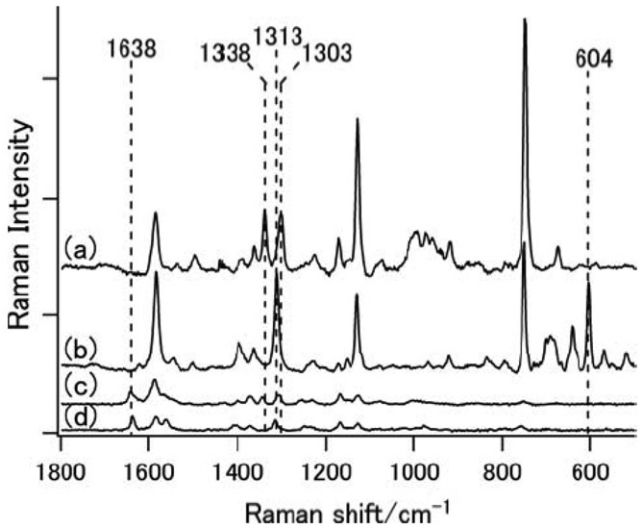

Fig. 7. Resonance Raman spectra (excited at 532 nm) of (a) reduced cytochrome *b*, (b) reduced cytochrome *c*, (c) oxidized cytochrome *b*, and (d) oxidized cytochrome *c*.[6]

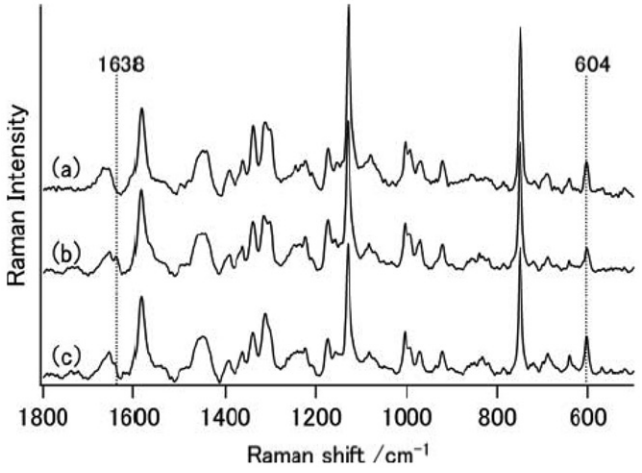

Fig. 8. Raman spectra (excited at 532 nm) of (a) living yeast-cell mitochondria, (b) isolated yeast mitochondria without ADP and succinate, and (c) isolated yeast mitochondria with ADP and succinate.[6]

mitochondria. Furthermore, the decrease in intensity of the oxidized forms on going from the inactive isolated mitochondria to the active mitochondria is evident from the decrease of the intensity of the peak at 1638 cm^{-1}, as well as by the increase in intensity of the peak at 604 cm^{-1}.

To quantify the redox-state changes of the cytochromes upon activation of the mitochondria, the difference spectrum, Fig. 8c minus Fig. 8b, is calculated as shown in Fig. 9a. In addition to the obvious changes in the two marker bands at 1638 cm^{-1} and 604 cm^{-1}, specific changes in the other cytochrome bands are clearly seen. By fitting this difference spectrum with a linear combination of the standard spectra of the reduced- and oxidized forms of cytochromes *b* and *c* (Fig. 7), it is now possible to quantitatively determine the coefficients that describe the redox-state changes of cytochromes that accompany the activation of mitochondrial respiration that is induced by the substrates. This is a first attempt towards the in vivo quantitation of mitochondrial respiration in a single living cell.

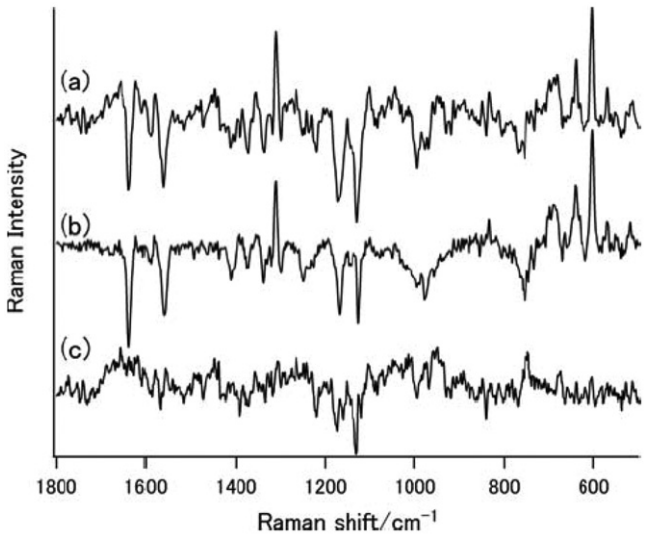

Fig. 9. (a) Difference spectrum of Fig. 8(c) minus Fig. 8(b), which shows the effect of ADP and succinate on the isolated mitochondria. (b) Best-fit linear combination of the four standard cytochrome spectra (Fig. 7) and (c) the residual spectrum. [6]

4.2. The 1602 cm^{-1} Band. The "Raman Spectroscopic Signature of Life" in Yeast

Figure 10 shows time- and space-resolved Raman spectra of a single living yeast cell that is treated with KCN. According to this experiment, the band at 1602 cm^{-1} starts to decrease in intensity immediately after the addition of KCN (3 min, Fig. 10b), continues becoming less intense (Fig. 10b and 10c), and then disappears completely after tens of minutes (35 min, Fig. 10e). The protein band at 1003 cm^{-1} remains constant, whilst the lipid bands gradually become less intense. The peak position of the CH bend changes from 1442 cm^{-1} (Fig. 6a) to 1447 cm^{-1} (Fig. 10e), together with a decrease in the band for the phospholipid head-group at 718 cm^{-1}. In the presence of cyanide, the function of cytochrome oxidase, which transfers an electron to the final electron-acceptor oxygen atom, is inhibited and, hence, the electron-transport process comes to a halt. Therefore, we infer that the band at 1602 cm^{-1} is associated with a molecule that is directly or indirectly related to mitochondrial respiration.

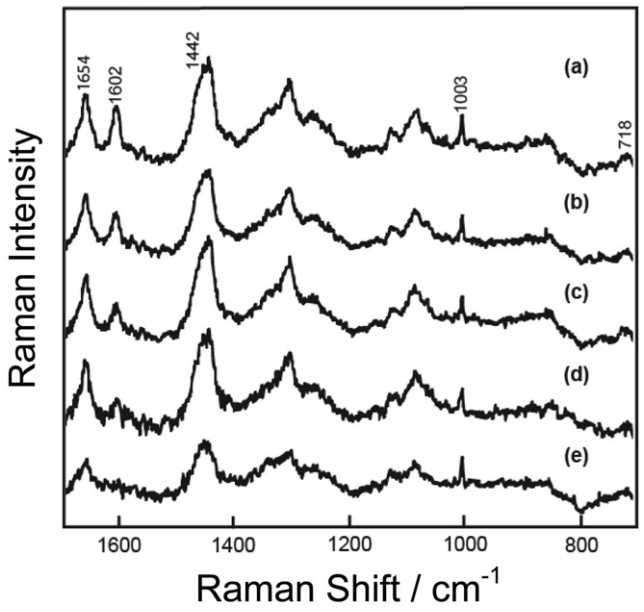

Fig. 10. (a) Raman spectra of living yeast mitochondria and after treatment with respiratory inhibitor potassium cyanide for (b) 3 min, (c) 10 min, (d) 20 min, and (e) 35 min.[3]

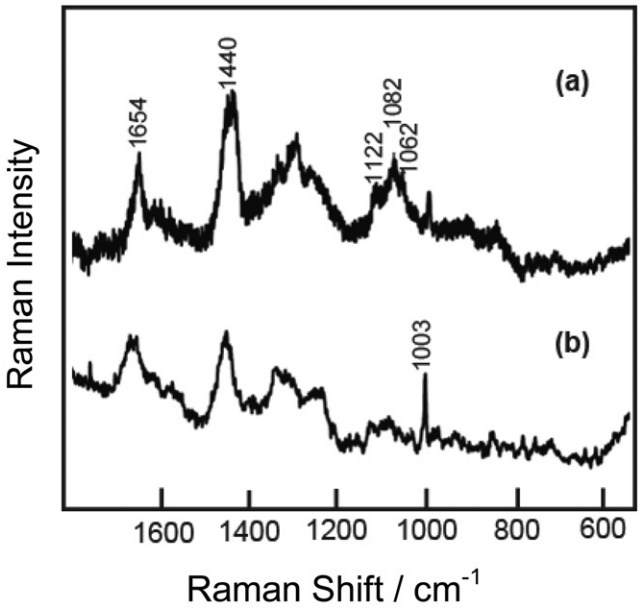

Fig. 11. Raman spectra of yeast that was cultured under anaerobic conditions for (a) 2 days and (b) 3 days.[33]

The band at 1602 cm^{-1} disappears when *S. pompe* is cultured in a 100 % nitrogen atmosphere (anaerobic conditions, Fig. 11). The disappearance of the band at 1602 cm^{-1} within two days (Fig. 11a) is followed by a decrease in the unsaturated lipid bands in the region 1000–1150 cm^{-1} on the third day (Fig. 11b) when compared with that of the intensities of the amide I (1660 cm^{-1}) and phenylalanine peaks (1003 cm^{-1}).[33] In addition, the ratio of the intensity of the *gauche* band (1082 cm^{-1}) to that of the *trans* bands (1062 and 1122 cm^{-1}) decreases with increasing duration of the anaerobic culture. This change suggests that the lipids are more rigid under oxygen-depleted conditions. It is a well-established fact that synthesis of long-chain unsaturated fatty acids requires the presence of oxygen.[34] Furthermore, mitochondrial activity is shown to be proportional to the level of unsaturated fatty acids.[35] Our observations on the lower levels of unsaturated fatty acids in anaerobic conditions correlates with the cellular physiology. A decrease in the levels of unsaturated fatty acids coupled with the absence of the band at 1602 cm^{-1} further strengthens our claim that it is an indicator of mitochondrial respiration.

Yeast that is cultured in a 100% oxygen atmosphere does not show the band at 1602 cm^{-1}, unlike yeast that is cultured in a 20% oxygen atmosphere (data not shown).[33] This effect is most-probably due to oxidative stress. To test this hypothesis, we used a cell-permeable oxidant, hydrogen peroxide, and measured time-resolved Raman spectra. The results are shown in Fig. 12 in the form of difference spectra. As expected, the peak

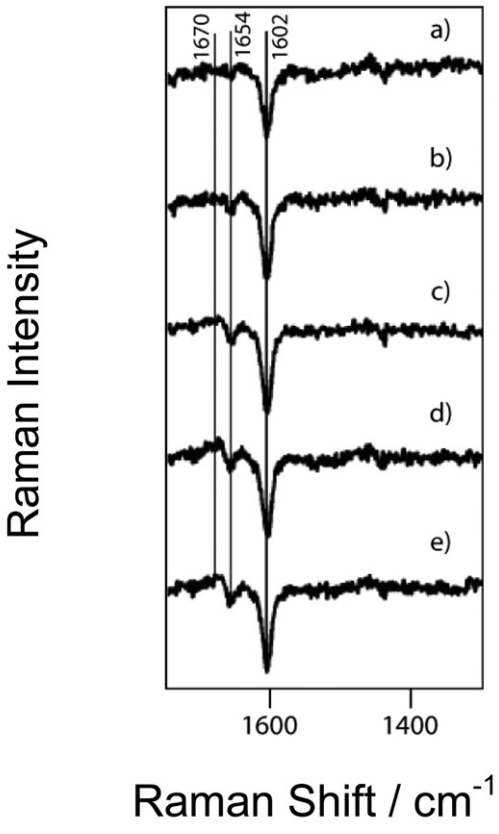

Fig. 12. Difference Raman spectra of living yeast after treatment with hydrogen peroxide for a) 1 min, b) 10 min, c) 15 min, d) 20 min, and e) 35 min.[33]

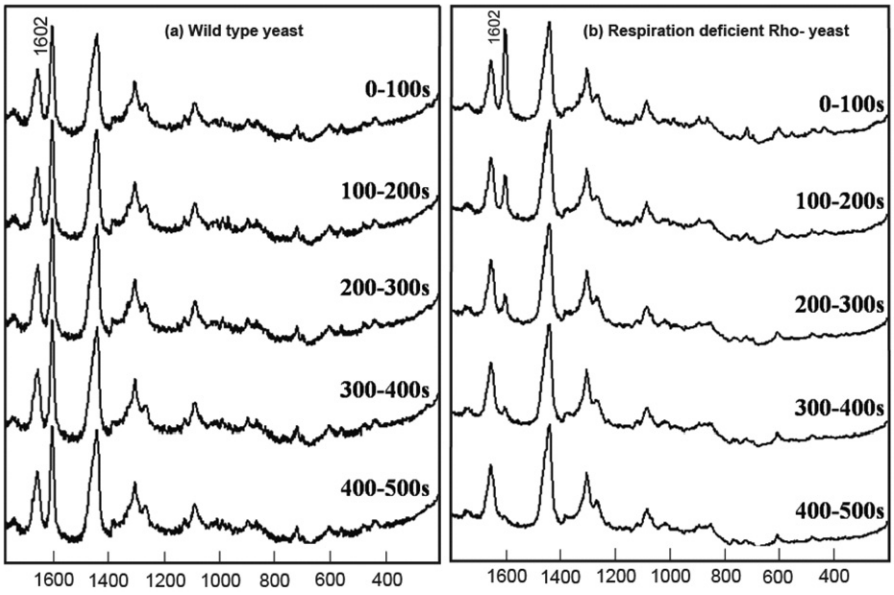

Fig. 13. Effect of laser irradiation at 632.8 nm on the 1602 cm^{-1} band in (a) wild-type- and (b) respiration-deficient Rho- yeast.[40]

at 1602 cm^{-1} disappears very quickly on treatment with hydrogen peroxide. In addition, a negative peak at 1654 cm^{-1} (C=C stretch of the *cis* C=C bond) and a positive shoulder at around 1670 cm^{-1} (*trans* C=C stretch) are observed.[36,37] This spectroscopic change indicates that a *cis*-to-*trans* conformation change is induced by the addition of hydrogen peroxide. Excess hydrogen peroxide generates free radicals, thereby leading to radical-mediated *cis*/*trans* isomerization of the lipids. High levels of *trans* fatty acids has been shown to decrease the respiratory activity of yeast.[38] This observation suggests that acute oxidative stress is likely to decrease mitochondrial activity by affecting its membrane lipids. The concomitant decrease in the intensity of the band at 1602 cm^{-1} is a response to the decline in mitochondrial activity.

A mutant yeast strain that is deficient in respiration has been studied to see its effect on the band at 1602 cm^{-1}. Rho- mutants possess truncated versions of the mitochondrial genome.[39] Because mitochondrial DNA codes for some of the components of the electron-transport-complex proteins, respiration is compromised in Rho- mutants. Fig. 13 shows two series of time-lapse Raman observations of the wild-type- (Fig. 13a) and Rho- strains (Fig. 13b) of budding yeast. The Rho- mutant that is cultured in aerobic conditions shows the band at 1602 cm^{-1}.[40] However, in this mutant, the band at 1602 cm^{-1} photo-bleaches on irradiation at 632.8 nm (Fig. 13b), in contrast to the wild-type strain, which shows no photo-bleaching (Fig. 13a). If the laser irradiation is blocked, then the mutant strain regains the 1602 cm^{-1} band. This difference in behavior between the wild-type- and the Rho- cells is most likely due the difference in their respiratory activity. From the observations on these rho- cells, cellular-respiration inhibitors, and the oxidative stress, we consider that the rate of the decrease in the intensity of the band at 1602 cm^{-1} reflects mitochondrial dysfunction that is induced under these conditions. Thus, it provides a quantitative measure of mitochondrial dysfunction in a single living cell.

Raman spectra of known biological molecules in mitochondria, such as cytochrome *a*, cytochrome *c*, ATP, ADP, FAD, and NAD, do not show the band at 1602 cm^{-1}. Therefore, isotope-substitution experiments have been carried out to assign the vibrational mode that gives rise to this band. Culturing yeast cells in a 20% $^{18}O_2$ environment did not show any peak-shift, thus implying that oxygen is not involved in this vibrational mode. Culturing with ^{13}C-substituted amino acids did not show any shift of the 1602 cm^{-1} band either. However, culturing the cells in ^{13}C- or ^{2}H-substituted D-glucose exhibited peak shifts (Fig. 14). ^{13}C substitution shifts the peak from 1602 cm^{-1} (Fig. 14a) to 1542 cm^{-1} (Fig. 14b), whilst ^{2}H substitution shifts it to 1599 cm^{-1} (Fig. 14a).[41] A ^{13}C shift of 60 cm^{-1} suggests that a C=C double bond is involved. A minimal shift of 3 cm^{-1} on ^{2}H substitution implies that the probable origin is a C=C double bond with no hydrogen atoms attached to it.

It is known that the semiubiquinone radical anion, an electron carrier in the mitochondrial electron-transport chain, shows a strong isolated Raman band at around 1600 cm^{-1}.[42] The 2,5-dichloro-p-benzosemiquinone radical anion also has a strong and sharp band at 1602 cm^{-1}.[43]

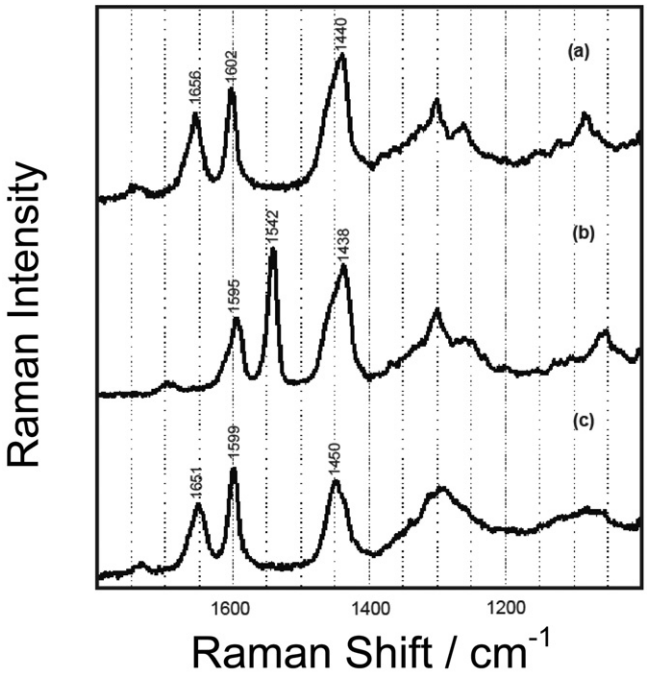

Fig. 14. Raman spectra of yeast cells that were grown in (a) an unsubstituted glucose medium, (b) a ^{13}C-substituted D-glucose medium, and (c) a deuterium-substituted D-glucose medium.[41]

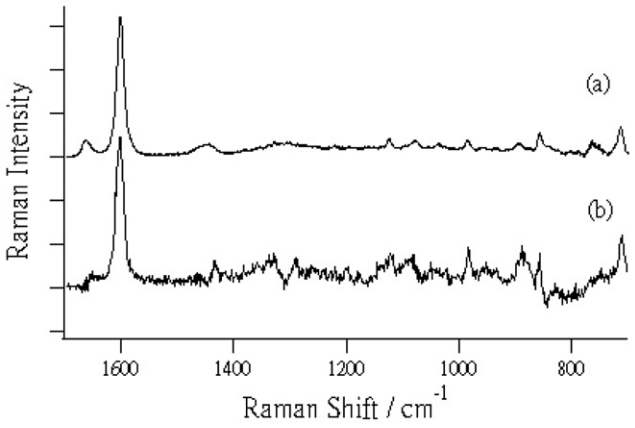

Fig. 15. Raman spectra of (a) a solution of ergosterol in $CHCl_3$ and (b) the depleting component in isolated mitochondria, whilst the 1602 cm^{-1} signature weakens on treatment with NaN_3.

These bands are assigned to in-phase stretching modes of the conjugated C=C bonds of the quinoid ring, which have no hydrogen atoms attached to them. From these facts, we assume that the semiubiquinone radical anion is a strong candidate for the origin of the band at 1602 cm^{-1}. This assumption accounts very well for the intriguing behavior of this band, which is most-probably related to mitochondrial dysfunction. Meanwhile, we have found that ergosterol, a fungal sterol, also shows a strong Raman band at 1602 cm^{-1} and that the depleting spectrum on treatment with NaN_3 agrees with that of ergosterol (Fig. 15).[26] It seems that this steroid molecule contributes significantly to the band at 1602 cm^{-1}. Ergosterol is known to exist in two forms in yeast cells. Free Ergosterol is a component of many organelle membranes, including mitochondria. Esterified Ergosterol is present in the lipid bodies of yeast. The assignment of the band at 1602 cm^{-1} to ergosterol is consistent with the isotope-substitution results, if we assume that the ^{2}H substitution is imperfect because of the exchange of hydrogen atoms. However, the high sensitivity of the intensity of the 1602 cm^{-1} band to external stresses is yet to be elucidated.

5. Dynamics of Cell-Death

When a yeast cell that is sandwiched between a cover glass and a slide glass (Vaseline-sealed to prevent drying) is microscopically monitored for several hours, it is likely to experience nutrient- and oxygen-deprivation stress. It is known that a dancing body, that is, a particle that shows vigorous Brownian motion, appears in the vacuole of such cells.[44] The Raman spectrum of the dancing body shows two strong peaks at 1160 cm^{-1} and 700 cm^{-1}. These two peaks match very well with those of crystalline sodium polyphosphate (data not shown). The dancing body contains substantial amount of crystalline polyP. We have found that, once a dancing body is formed inside the vacuole of a starving *S.cerevisiae* cell, it eventually shrinks and the cell subsequently dies. This spontaneous death process of starving budding yeast is studied with the time-resolved Raman-mapping experiments (Fig. 16). Between 0 min and 5 h 50 min, the cell is in its normal state. The "Raman spectroscopic signature of life" at 1602 cm^{-1} shows a high intensity, along with those of the lipids (1440 cm^{-1}) and proteins (1002 cm^{-1}) that are localized outside the vacuole. At 6 h, a dancing body suddenly appears and, at the same time, the "Raman spectroscopic signature of life" becomes very weak. As discussed earlier, the rate of decline in the intensity of the 1602 cm^{-1} peak likely reflects the degree of acute mitochondrial dysfunction that is brought about by nutrient-deprivation stress. At 8 h 41 min, the peak at 1602 cm^{-1} disappears completely but the distribution of the lipids and proteins still remains unchanged. At 9 h and 31 min and later, the vacuole disappears and the molecular distribution becomes random, thus indicating that the cell is not living any more. Many cells have been studied to show the disappearance of the band at 1602 cm^{-1} and the concomitant appearance of a dancing body.[45] Eventually, the dancing body also disappears, the vacuole shrinks, and cell-death is imminent. The lipid peak at 1440 cm^{-1} and the phenylalanine peak at 1002 cm^{-1} do not show changes until the sub-cellular morphology disintegrates.

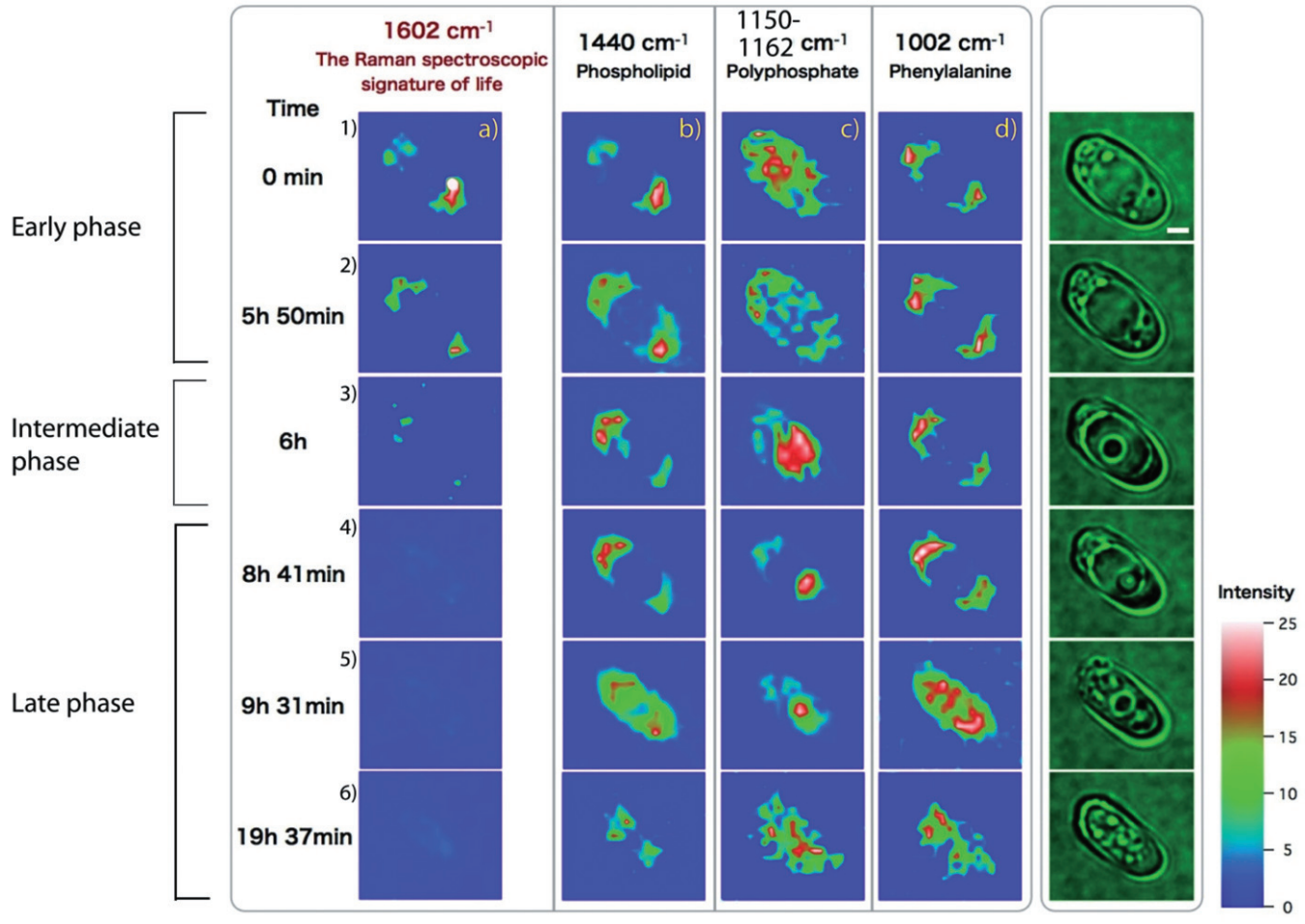

Fig. 16. Raman mapping of starvation-induced cell-death.

This response of yeast to starvation is divided into three sequential phases: the early phase, the intermediate phase, and the late phase.

In the early phase, the intensity of the band at 1602 cm^{-1} gradually decreases (Fig. 16, left-hand column, row 1 → row 2), thus indicating a slow-onset mitochondrial dysfunction. Concomitantly, the concentration of vacuolar polyP decreases, most-probably due to hydrolysis (Fig. 16, third column, row 1 → row 2). The size of the vacuole remains unchanged in this phase. The vacuolar polyP concentration is known to be coupled with the energetic state of the cell.[46] In the presence of 2-deoxy glucose, there is a decrease in the cellular ATP content and a simultaneous decrease in vacuolar polyP and decrease in the cytoplasmic pH value.[47,48] Mitochondrial uncouplers and vacuolar H+-ATPase inhibitors also lead to hydrolysis of the vacuolar polyP.[48] These NMR-based studies correlate well with our direct in vivo observation of the decrease in vacuolar polyP during starvation. The hydrolysis of vacuolar polyP sustains the cellular ATP concentration during this phase. The hydrolysis of polyP is likely to increase the concentrations of $H_2PO_4^-$ and HPO_4^{2-} in the vacuole and in the cytoplasm.

In the intermediate phase response to starvation, there is a sudden decrease and disappearance of the band at 1602 cm^{-1} (Fig. 16, left-hand column, row 3) and a concomitant appearance of a dancing body in the vacuole (Fig. 16, third column, row 3). This result implies a rapidly progressing mitochondrial dysfunction, followed by the appearance of insoluble polyP inside the vacuole. We note a laser-trapping effect of crystalline polyP that results in apparent spreading of the distribution of polyP band inside the vacuole. By using optical imaging, we observe the formation of a small granule on the inner aspect of the vacuolar membrane. This granule gradually increases in size, detaches from the membrane, and appears as a dancing body in the middle of the vacuole. The formation of the dancing body indicates the presence of insoluble calcium polyP. The solubility of polyP decreases owing to the rise in free

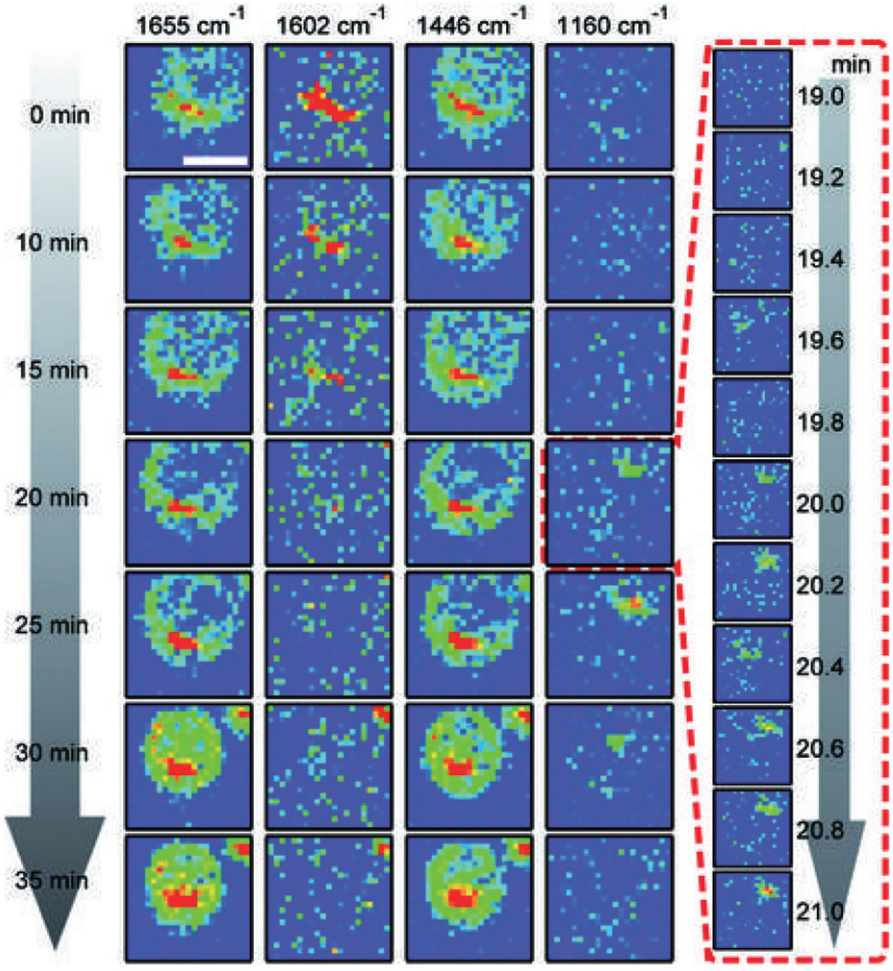

Fig. 17. CARS imaging of Raman bands during laser-induced cell-death.

calcium and simultaneous drop in polyP concentration during starvation. The size of the vacuolar is enlarged in the intermediate phase response to starvation. This increase in the size of the vacuole is supportive of the energetic failure caused by mitochondrial dysfunction. In addition to the respiratory function, mitochondria maintain cellular calcium homeostasis and can accumulate large amounts of calcium.[49–51] The stored calcium is rapidly released during mitochondrial permeability transition.[52] The rapid decline in the intensity of the peak at 1602 cm^{-1} probably indicates the occurrence of a mitochondrial permeability transition (MPT) that precedes necrotic or apoptotic cell-death.[53,54] The ability of mitochondria to maintain cellular ATP and calcium homeostasis is completely compromised.

In the late phase of nutrient deprivation, there is a decrease in the intensity of vacuolar polyP (Fig. 16, third column, row 4 → row 6). The vacuole initially decreases in size and, later, starts to disintegrate. In its energy-depleted state, the levels of polyP are inadequate to sequester free calcium ions in its soluble form. This inadequacy leads to an increase in free calcium in the vacuole and in the cytoplasm. The excess of free calcium causes membrane damage. Thus, we see lysis of the vacuole owing to the osmotic pressure of inorganic ions and other vacuolar content, along with the damage to the vacuolar membrane that is caused by calcium in an energy-depleted state. We also find a random distribution of the proteins (Fig. 16, fourth column, rows 5 and 6) and unhydrolyzed vacuolar polyPs (Fig. 16, third column, rows 5 and 6). The loss of cellular architecture is suggestive of necrotic cell-death caused by the release of lytic enzymes from the vacuole. A similar sequence of subcellular events is observed in cultured rat hepatocytes: lysosomal disintegration follows MPT in energy-deprived hepatocytes.[55] The importance of lysosome in cell-death is increasingly being recognized.[56,57] From our

study, we infer a functional cross-talk between mitochondria, the molecule giving rise to the band at 1602 cm^{-1}, and the yeast vacuole in regulating cell-survival and cell-death. There is additional inference on the role of vacuolar polyP in preventing calcium-mediated necrotic cell-death.

Cell-death that is caused by laser irradiation has been studied by using coherent anti-Stokes Raman scattering (CARS) microspectroscopy.[58] This experiment shows a better time-resolution than the previous spontaneous Raman experiments and demonstrates that the disappearance of the 1602 cm^{-1} band precedes the appearance of polyphosphate during cell-death (Fig. 17). Thus, an association between the 1602 cm^{-1} Raman band and life is once-again confirmed by another technique, thereby further justifying our terminology "the signature of life".

Conclusions

By using Raman microspectroscopy, we have traced three fundamental biological processes in a living yeast cell, namely, cell division, respiration, and cell death, by means of physical chemistry. The capability of in vivo Raman studies of living cells is thus established beyond doubt. We have suggested that the 1602 cm^{-1} band, which is known as the "Raman spectroscopic signature of life", gives a measure of mitochondrial dysfunction, whilst the cytochrome resonance Raman bands have the capability to quantify the respiration activity of a single cell. By using different Raman excitation wavelengths, we are able to highlight different biomolecules by using the resonance Raman effect: excitation at 632.8 nm for lipids and at 532 nm for cytochromes. The dynamics of starvation-induced cell-death have been interpreted in terms of "cross-talk" between the vacuole and the molecule, thereby giving rise to the signature at 1602 cm^{-1}. Mitochondria are likely to be involved in this cross-talk through a calcium-mediated signaling process. This Personal Account has demonstrated that biomolecules, such as proteins, lipids, polyphosphates, sugars, and so on, give rise to Raman signatures that are highly useful for the in vivo analysis of living cells at the molecular level. These signatures are obtainable without the need for any pre-treatments, such as tagging or gene manipulation. With further advancement in the instrumentation, Raman microspectroscopy will shed much more physicochemical light on various biological processes in living cells and will establish a new discipline that may well be called "living-cell physical chemistry".

Acknowledgements

The authors would like to thank all of their collaborators in the work presented herein, in particular, Drs. Yu-san Huang, Yasuaki Naito, Liang-da Chiu, Chikao Onogi, and Minoru Kakita, whose DSc theses provide the material for the main body of this review.

REFERENCES

[1] G. J. Puppels, F. F. de Mul, C. Otto, J. Greve, M. Robert-Nicoud, D. J. Arndt-Jovin, T. M. Jovin, *Nature* **1990**, *347*, 301–303.
[2] Y. Huang, T. Karashima, M. Yamamoto, H. Hamaguchii, *J. Raman Spectrosc.* **2003**, *34*, 1–3.
[3] Y. Huang, T. Karashima, M. Yamamoto, H. Hamaguchi, *Biochemistry* **2005**, *44*, 10009–10019.
[4] Y. Huang, T. Karashima, M. Yamamoto, T. Ogura, H. Hamaguchi, *J. Raman Spectrosc.* **2004**, *35*, 525.
[5] C. Onogi, H. Hamaguchi, *Chem. Lett.* **2010**, *39*, 270–271
[6] M. Kakita, V. Kaliaperumal, H. O. Hamaguchi, *J. Biophotonics* **2012**, *5*(*1*), 20–24.
[7] S. FORSBURG, P. NURSE, *Annu. Rev. Cell Biol.* **1991**, *7*, 227–256.
[8] J. H. Duffus, *Method. Cell Biol.* **1975**, *12*, 77–97.
[9] P. R. Carey, *Biochemical applications of Raman and resonance Raman spectroscopies*. Academic Press, New York, **1982**, pp. xi, 262.
[10] K. Larsson, R. P. Rand, *Biochim. Biophys. Acta* **1973**, *326*, 245–255.
[11] M. N. Siamwiza, R. C. Lord, M. C. Chen, T. Takamatsu, I. Harada, H. Matsuura, T. Shimanouchi, *Biochemistry* **1975**, *14*, 4870–4876.
[12] Y. Xie, D. Zhang, G. K. Jarori, V. J. Davisson, D. Ben-Amotz, *Anal. Biochem.* **2004**, *332*, 116–121.
[13] S. A. Overman, K. L. Aubrey, N. S. Vispo, G. Cesareni, G. J. Thomas, Jr., *Biochemistry* **1994**, *33*, 1037–1042.
[14] H. Deng, V. A. Bloomfield, J. M. Benevides, G. J. Thomas, Jr., *Biopolymers* **1999**, *50*, 656–666.
[15] P. Nurse, *Nature* **1990**, *344*, 503–508.
[16] S. Atherton-Fessler, G. Hannig, H. Piwnica-Worms, *Book Reversible tyrosine phosphorylation and cell cycle control*, Editor, City, **1993**, Vol. *4*, p. 433.
[17] G. Draetta, H. Piwnica-Worms, D. Morrison, B. Druker, T. Roberts, D. Beach, *Nature* **1988**, *336*, 738–744.
[18] M. Dauchez, P. Derreumaux, P. Lagant, G. Vergoten, M. Sekkal, P. Legrand, *Spectrochim. Acta A* **1994**, *50*, 87–104.
[19] M. Dauchez, P. Lagant, P. Derreumaux, G. Vergoten, M. Sekkal, B. Sombret, *Spectrochim. Acta A* **1994**, *50*, 105–118.
[20] Y. Takai, T. Masuko, H. Takeuchi, *Biochim. Biophys. Acta* **1997**, *1335*, 199–208.
[21] J. L. Lippert, W. L. Peticolas, *P. Natl. Acad. Sci. USA.* **1971**, *68*, 1572–1576.
[22] R. G. Snyder, *J. Chem. Phys.* **1967**, *47*, 1316.
[23] M. Tasumi, T. Shimanouchi, *J. Mol. Spectrosc.* **1962**, *9*, 261.
[24] D. P. Cherney, J. C. Conboy, J. M. Harris, *Anal. Chem.* **2003**, *75*, 6621–6628.
[25] B. P. Gaber, W. L. Peticolas, *Biochim. Biophys. Acta* **1977**, *465*, 260–274.

[26] L.-da Chiu, F.H. Matsuda, T. Kobayashi, H. Torii and H.O. Hamaguchi, *J. Biophotonics*, in press.
[27] R. Zahedi, A. Sickmann, A. Boehm, C. Winkler, N. Zufall, B. Schonfisch, B. Guiard, N. Pfanner, C. Meisinger, *Mol. Biol. Cell* **2006**, *17*, 1436–1450.
[28] L.-d. Chiu, M. Ando, H.-o. Hamaguchi, *J. Raman Spectrosc.* **2010**, *41*, 2–3.
[29] R. Okamitsu, T. Shimizu, T. Nagata, H. Hamaguchi, *Proceedings of the XXI International Conference on Raman Spectroscopy*, London, **2008**, 890.
[30] H. Tang, H. Yao, G. Wang, Y. Wang, Y. Q. Li, M. Feng, *Opt. Express* **2007**, *15*, 12708–12716.
[31] V. V. Pully, C. Otto, *J. Raman Spectrosc.* **2009**, *40*, 473–475.
[32] K. Hamada, K. Fujita, N. Smith, M. Kobayashi, Y. Inouye, S. Kawata, *J. Biomed. Opt.* **2008**, *13*, 044027.
[33] Y. S. Huang, T. Nakatsuka, H. O. Hamaguchi, *Appl. Spectrosc.* **2007**, *61*, 1290–1294.
[34] C. E. Martin, C. S. Oh, Y. Jiang, *Biochim. Biophys. Acta* **2007**, *1771*, 271–285.
[35] S. Marzuki, G. S. Cobon, J. M. Haslam, A. W. Linnane, *Arch. Biochem. Biophys.* **1975**, *169*, 577–590.
[36] J. E. D. Davies, F. D. Gunstone, J. A. Barve, I. A. Ismail, P. Hodge, *J. Chem. Soc. Perkins Trans. 2* **1972**, 1557–1561.
[37] G. F. Bailey, R. J. Horvat, *J. Am. Oil Chem. Soc.* **1972**, *49*, 494.
[38] B. S. Tung, E. R. Unger, B. Levin, T. A. Brasitus, G. S. Getz, *J. Lipid Res.* **1991**, *32*, 1025–1038.
[39] V. Contamine, M. Picard, *Microbiol. Mol. Biol. Rev.* **2000**, *64*, 281–315.
[40] C. Onogi, H. O. Hamaguchi, *J. Phys. Chem. B* **2009**, *113*, 10942–10945.
[41] C. Onogi, H. Torii, H. O. Hamaguchi, *Chem. Lett.* **2009**, *38*, 898–899.
[42] X. J. Zhao, T. Ogura, M. Okamura, T. Kitagawa, *J. Am. Chem. Soc.* **1997**, *119*, 5263–5264.
[43] G. N. R. Tripathi, R. H. Schuler, *J. Chem. Phys.* **1982**, *76*, 2139–2146.
[44] Y. Naito, A. Toh-e, H. Hamaguchi, *J. Raman Spectrosc.* **2005**, *36*, 837–839.
[45] J. Laane, *Frontiers of Molecular Spectroscopy*, Elsevier, **2009**.
[46] K. Y. Chen, *Prog. Mol. Subcell. Biol.* **1999**, *23*, 253–273.
[47] M. C. Loureiro-Dias, H. Santos, *FEMS Microbiol. Lett.* **1989**, *57*, 25–28.
[48] B. Beauvoit, M. Rigoulet, G. Raffard, P. Canioni, B. Guerin, *Biochemistry* **1991**, *30*, 11212–11220.
[49] M. R. Duchen, *Cell Calcium* **2000**, *28*, 339–348.
[50] M. R. Duchen, *J. Physiol.* **2000**, *529*, 57–68.
[51] G. Szabadkai, M. R. Duchen, *Physiology Bethesda* **2008**, *23*, 84–94.
[52] P. Bernardi, V. Petronilli, *J. Bioenerg. Biomembr.* **1996**, *28*, 131–138.
[53] J. Lemasters, A. Nieminen, T. Qian, L. Trost, S. Elmore, Y. Nishimura, R. Crowe, W. Cascio, C. Bradham, D. Brenner, *BBA-Bioenergetics* **1998**, *1366*, 177–196.
[54] J. Lemasters, T. Qian, C. Bradham, D. Brenner, W. Cascio, L. Trost, Y. Nishimura, A. Nieminen, B. Herman, *J. Bioenerg. Biomembr.* **1999**, *31*, 305–319.
[55] G. Zahrebelski, A. Nieminen, K. Al-Ghoul, T. Qian, B. Herman, J. Lemasters, *Hepatology* **1995**, *21*, 1361–1372.
[56] M. Guicciardi, M. Leist, G. Gores, *Oncogene* **2004**, *23*, 2881–2890.
[57] T. Kirkegaard, M. Jäättelä, *BBA-Mol. Cell Res.* **2009**, *1793*, 746–754.
[58] M. Okuno, H. Kano, P. Leproux, V. Couderc, J. P. Day, M. Bonn, H.O. Hamaguchi, *Angew. Chem. Int. Edit.* **2010**, *49*, 6773–6777.

